npj | science of food

Article

Published in partnership with Beijing Technology and Business University

https://doi.org/10.1038/s41538-024-00333-3

Identification strategy of wild and cultivated Astragali Radix based on REIMS combined with two-dimensional LC-MS

Sijian Chen[1], Xiaoshuang Li[1], Danshu Shi[2], Yisheng Xu[3], Yingyuan Lu[1] ✉ & Pengfei Tu[1] ✉

A rapid and real-time method was established based on the combination of rapid evaporative ionization mass spectrometry (REIMS) and two-dimensional liquid chromatography mass spectrometry (2DLC-MS) for identification of wild Astragali Radix (WAR) and cultivated AR (CAR). The samples were analyzed under ambient ionization without time-consuming sample preparation. The phenotypic data of WAR and CAR were used to develop a real-time recognition model. Subsequently, the compounds in these two species were comprehensively characterized based on 2DLC-MS, and 45 different compounds were screened out by multivariate statistical analysis. A semi-quantitative method for 45 different compounds was established based on ultrahigh-performance liquid chromatography/quadrupole-linear ion trap mass spectrometry (UHPLC-QTRAP-MS). The results showed that the relative content of most compounds in WAR was higher than in CAR. In summary, the method has demonstrated remarkable performance in distinguishing between WAR and CAR, providing a reference in the field of traditional Chinese medicine (TCM) analysis and identification.

Astragali Radix (AR), the dried root of *Astragalus membranaceus* (Fisch.) Bge. var. *monghoicus* (Bge.) Hsiao (AMM) or *Astragalus membranaceus* (Fisch.) Bge. (AM), is one of the most popular TCMs worldwide[1]. AR, mainly produced in Gansu, Shanxi, and Inner Mongolia provinces of China, contains primarily chemical constituents such as saponins, flavonoids, organic acids and polysaccharides[2]. Up to now, AR has been proven to have a wide range of biological functions, including immunomodulatory, antioxidative and anti-diabetic activities, so it is widely used in medicine and favored by people[3]. At present, the mainstream variety of AR on the market is AMM, and the main circulating AR commodities are WAR and CAR. Nevertheless, the supply of wild AR resources is gradually decreasing, failing to satisfy the escalating demand. At the same time, the success and popularization of AR cultivation techniques have resulted in the influx of CAR into the market, leading to the phenomenon of mixing the two[4]. Related studies have shown that there are differences in chemical components between WAR and CAR, which may result in changes in clinical efficacy and dose-effect relationship[5]. Therefore, it is of great significance to establish a rapid and effective method for identifying WAR and CAR.

In recent years, the development of spectroscopy, chromatography, and mass spectrometry (MS) has provided a new method for more accurate authentication. Spectroscopic techniques, including Raman, infrared and ultraviolet-visible spectroscopy, can obtain characteristic information through the interaction between matter and light[6]. Chromatography and MS techniques mainly include high performance liquid chromatography (HPLC), thin layer chromatography (TLC), liquid chromatography-mass spectrometry (LC-MS) and gas chromatography-mass spectrometry (GC-MS), which are commonly used to identify plant ingredients[7], environmental pollutants[8], drug residues[9], illegal food additives[10] and pesticides[11]. LC-MS is an analytical method combining LC and MS. Unlike HPLC, LC-MS utilizes MS as a detector and can provide a wealth of accurate information in a short period of time. As a result, it has become the primary method for identifying easily-confused plants in literature[12]. Additionally, targeted and nontargeted strategies in MS have also been applied in the field of plant metabolomics to distinguish plant phenotypes, and the analytical workflow has been described comprehensively[13]. However, these techniques have some limitations, such as the need for cumbersome sample preparation and time-consuming instrument operation. Furthermore, these techniques can not fully characterize the samples, leading to insufficient discrimination accuracy.

REIMS is an ambient ionization MS technique introduced by Professor Takats' team in 2013[14]. REIMS utilizes an innovative hand-held sampling technology that eliminates the need for a laborious sample preparation or chromatographic separation process by cutting molecules on the surface of the sample to form an aerosol, which is guided through a catheter and

[1]State Key Laboratory of Natural and Biomimetic Drugs, School of Pharmaceutical Sciences, Peking University, Beijing, China. [2]Shimadzu (China) Co., Ltd., Beijing Branch, Beijing, China. [3]Waters Technology(Beijing) Co., Ltd., Beijing, China. ✉e-mail: luyingyuan518@bjmu.edu.cn; pengfeitu@bjmu.edu.cn

aspirates the analyte-containing vapor to a mass spectrometer for analysis[15]. This technique has a fast analysis speed, and it takes only a few seconds from sample cutting to data generation. It can be used to detect chemical substances in samples under atmospheric conditions, and identify key attributes as a "fingerprint", reflecting the species, quality or phenotypic characteristics of samples. Compared with traditional analytical methods, REIMS could achieve real-time and low-cost analysis without sample preparation and pre-separation[16,17]. Therefore, REIMS demonstrate great advantages in real-time phenotyping and species differentiation[18]. REIMS was initially applied in the medical field, such as the identification of tissue type, the detection of breast cancerous tissues, the screening of cervical cancer, the distinction between benign tumors and malignant tumors and others[19–21]. In recent years, REIMS has also been widely used for rapid detection of food quality and safety, such as the detection of tuna meat, fish, shrimp, and beer[22–25].

Two-dimensional liquid chromatography (2DLC) is a highly promising separation technique that could significantly enhance separation capability and resolution. The combination of cation-exchange, size exclusion or hydrophilic interaction chromatography with reversed-phase chromatography could produce ideal orthogonality and high peak capacity[26,27]. The components that are difficult to separate using one-dimensional chromatography can usually be well separated in 2D chromatography[28]. Therefore, different combinations of 2DLC are increasingly used in high-throughput metabolomics analysis to expand the coverage of metabolites and improve peak capacity. In addition, QTRAP-MS has attracted more and more attention in sample analysis due to its multi-scanning capabilities handled by triple quadrupole (QQQ) and linear ion trap, including multiple ion monitoring (MIM), multiple reaction monitoring, precursor ion scan, neutral loss scan, enhanced mass scan, is the full list of instrument capabilities needed in any case, these sorts of abilities are generally widely accepted with modern QQQ/QTRAP instruments[29,30]. Numerous documents are currently available that utilize MS to analyze AR for type classification and quality control. For instance, Cai et al. used a diagnostic ions-guided method based on UPLC-QTOF/MS profiling to accurately trace AR species[31]. Zhao et al. established an off-line three-dimensional liquid chromatography system to analyze two AR species (AMM; AM). A total of 513 compounds were characterized from two AR species, including 236 flavonoids, 150 riterpenoids, 18 organic acids, and 109 others compounds[32]. However, given the compositional complexity of most herbal metabolites, the aforementioned single analytical method is not sufficient to completely characterize complex components and trace components. Therefore, an integrated strategy combining different MS instruments could provide a solid foundation for the systematic characterization and annotation of the chemical diversity of TCM.

The present study aimed to develop a method that could rapidly and accurately distinguish between WAR and CAR based on REIMS combined with 2DLC-MS technology. REIMS was used to establish a discriminant model to identify unknown AR samples in the market, thereby enabling accurate distinction of the two types. Subsequently, many batches of AR samples were characterized by 2DLC-MS, and potential markers were screened by multivariate statistical analysis to further verify the REIMS results. In addition, a QTRAP-MS platform was used to further screen potential markers and conduct semi-quantitative analysis. In this study, the REIMS method was developed to identify WAR and CAR in real time without any sample preparation. This study provides a rapid and almost nondestructive method for the qualitative detection of TCMs that are easily confused.

Results and discussion

The schematic diagram of this study was shown in Fig. 1, divided into three parts. Firstly, REIMS was used to identify WAR and CAR, and the working principle of REIMS was shown in Fig. 1a. Radiofrequency electrical current was directly applied to the AR samples through the iKnife. The sample was rapidly heated, releasing gas phase ions of metabolites into the vapor. Then, the vapor was drawn into the mass spectrometer via the sample transfer tube for MS analysis. The aerosol produced by burning the sample was found to contain significant gas-phase ions. Subsequently, a method based on a multivariate model to distinguish WAR and CAR was successfully established and was used for real-time identification of AR samples. Secondly, to further support the results obtained by the REIMS method, 2DLC-MS analysis was applied to verify the chemical composition-based differentiation between the two samples (Fig. 1b). 2DLC-MS was used to qualitatively analyze the samples of WAR and CAR, and differential compounds between WAR and CAR were identified through a multivariate statistical analysis model. Finally, using the MIM mode of QTRAP-MS, the potential markers were further screened and semi-quantified (Fig. 1c).

Optimization of REIMS experimental conditions

To achieve optimal ionization efficiency, critical parameters of REIMS were optimized using QC samples, including heater bias and cone voltage. The cone voltage was optimized from 30 V to 60 V, with signal intensity increasing as the voltage increased from 30 V to 40 V, reaching a maximum at 40 V. When the cone voltage exceeded 40 V, the intensity values significantly decreased (Fig. S1), possibly due to excessive sample evaporation and ionization caused by the high voltage. Hence, 40 V was selected as the optimal cone voltage. Similarly, the optimization of the heater bias was conducted from 40 V to 60 V (Fig. S2). It was found that the overall intensity of the total ion chromatograms (TICs) increased from 30 V to 55 V, then significantly decreased, resulting in the maximum signal intensity at a heater bias voltage of 55 V. Therefore, 40 V and 55 V were chosen as the optimal cone voltage and heater bias voltage, respectively.

REIMS identification of the WAR and CAR

The mass spectra of AR samples were obtained by REIMS in negative ion mode. To provide enough spectra to establish a statistical model, a comprehensive collection of 40 AR samples was amassed, consisting of 20 WAR and 20 CAR. Each AR sample was treated by iKnife and repeatedly cut 10 times. The relative standard deviation (RSD) values of ten chromatographic peak intensities of each sample are listed in Table S1. Overall, the RSD values are less than 15%, indicating minimal variability among the burn-to-burn variation in samples. These samples were used to create typical REIMS multispectral "fingerprints". Through precise mass measurements and corroboration with existing literature[32], 36 compounds within the mass spectra of WAR and CAR were detected and preliminarily characterized, encompassing organic acids, flavonoids, saponins, and other compounds. A detailed summary of the potential attribution information derived from the AR analysis is summarized in Table 1. The representative TICs and mass spectra were shown in Fig. 2a–d. The peaks were mainly located at *m/z* 100–500 and *m/z* 600–1000. Specifically, in the region of *m/z* 100–500 (Fig. 2c, d), compounds with *m/z* 113.0, 137.0, 255.1, 279.2, 341.1 and 455.4 ion peaks were observed in the mass spectra of both WAR and CAR. Among them, *m/z* 255.1, 279.2, 341.1 were attributed to liquiritigenin, linoleic acid and sucrose, as summarized in Table 1. In the region of *m/z* 600-900 (Fig. 2c, d), 10 saponins were preliminarily identified, with a mass error of ≤2.80 ppm, including astragaloside III, astragaloside II, astragaloside VI, agroastragaloside IV, etc, as enumerated in Table 1. Further exploration of these spectra demonstrated that obvious differences were observable in either the *m/z* 100–500 or *m/z* 600–1000 mass ranges. In the *m/z* 100–900 region (Fig. 2c, d), the great diversity of ion peaks was attributed to *m/z* 311.2, 383.4, 659.6, 683.3, 671.6, 768.7 and 976.8. The data of WAR was notably clear and informative, showing high intensity spectrum in the range of *m/z* 100–500. These differences between WAR and CAR could be attributed to the AR living conditions and detection techniques employed. These may be important for distinguishing WAR from CAR in the model. Additionally, the mass drift was corrected based on the reference peak of leucine enkephalin at *m/z* 554.3.

Multivariate statistical analysis

400 REIMS spectra were obtained from identified AR samples, comprising 20 from WAR and 20 from CAR, and were processed by LiveID software for the construction of stoichiometric model. As an unsupervised

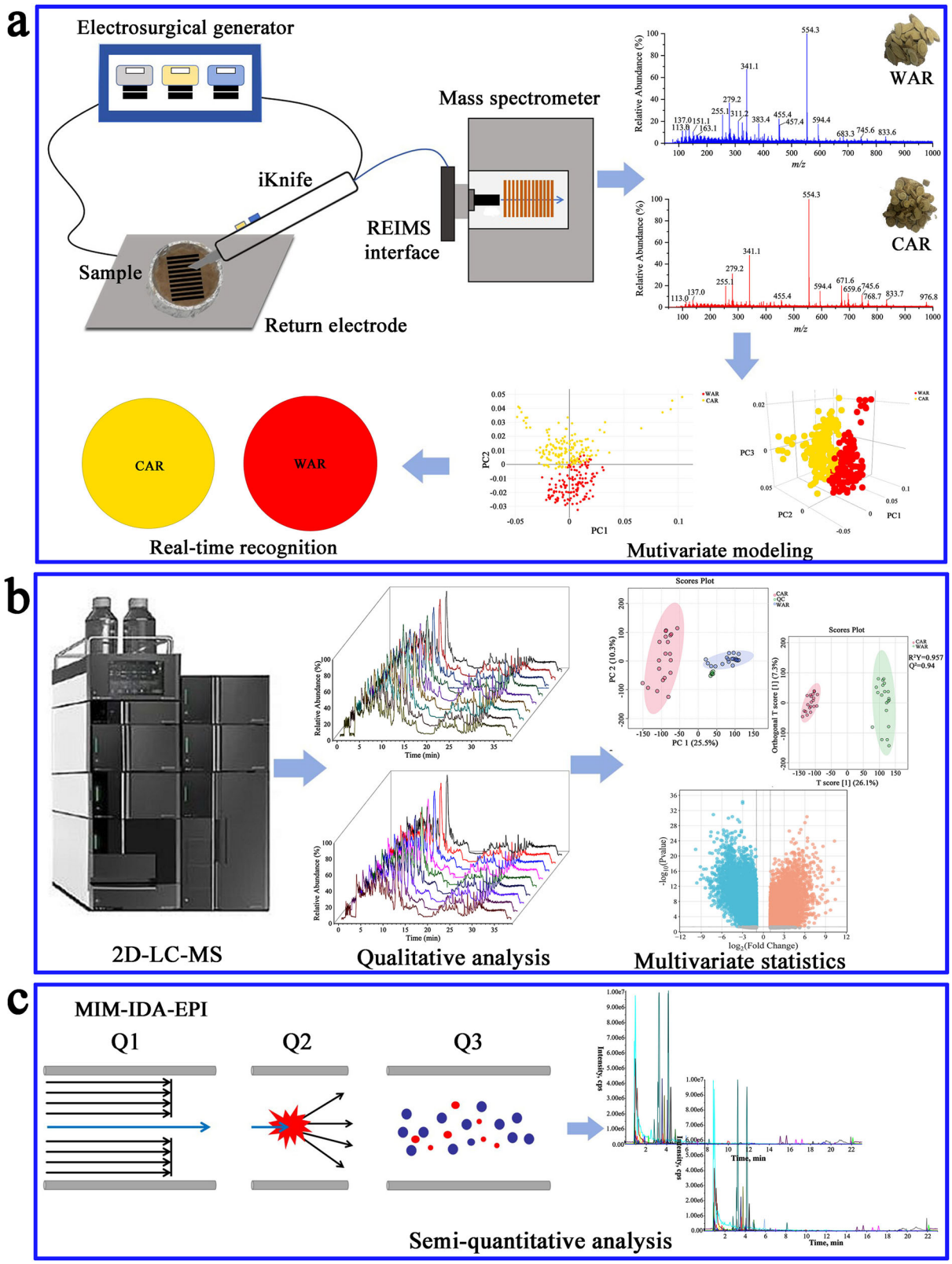

Fig. 1 | Experimental workflow of the study. a REIMS ion source and transfer setup. **b** 2DLC-MS characterization. **c** QTRAP-MS semi-quantitative analysis.

dimensionality reduction algorithm, PCA maximizes the variance in datasets by ignoring class labels and finding principal components. The PCA score plot (Fig. 3a) revealed tightly clustered WAR and CAR samples, indicating that the analytical strategy remained stable during the whole batch. A clear separation between the two groups was observed, suggesting significantly different compound profiles. Linear discriminant analysis (LDA) is a supervised data analysis technique that maximizes separation among multiple categories while minimizing differences within them. Combining unsupervised PCA with supervised LDA can reduce the chance of overfitting that may occur with a pure LDA model. Therefore, a PCA-

Table 1 | The probable attributions of compounds in WAR and CAR

Measured *m/z*	Theoretical *m/z*	Error (ppm)	Probable attribution
131.0442	131.0451	−6.9	L-asparagine
134.0456	134.0461	−3.7	Adenine
136.0399	136.0393	4.4	Trigonelline
146.0443	146.0447	−2.7	Glutamic acid
154.0613	154.0611	1.3	L-histidine
161.0244	161.0233	6.8	7-Hydroxycoumarin
163.0395	163.0389	3.7	Coumaric acid
164.0715	164.0706	5.5	L-phenylalanine
165.0540	165.0546	−3.6	3-Phenyllactic acid
167.0332	167.0338	−3.6	Vanillic acid
173.0093	173.0081	6.9	Aconitic acid
179.0548	179.0550	−1.1	D-Glucose
191.0182	191.0186	−2.1	Citric acid
253.0481	253.0495	−5.5	3',4'-Dihydroxyflavone
255.0654	255.0652	0.8	Liquiritigenin
267.0629	267.0652	−8.6	Formononetin
271.0604	271.0601	1.1	Naringenin
279.2335	279.2319	5.7	Linoleic acid
283.0622	283.0601	7.4	Biochanin A
297.0757	297.0758	−0.3	3-Hydroxy-3',4'-Dimethoxyflavone
299.0911	299.0914	−1.0	Methylnissolin
315.0850	315.0863	−4.1	3',4'-Dihydroxy-5,7-dimethoxyisoflavone
341.1059	341.1078	−5.6	Sucrose
417.1151	417.1180	−7.0	Liquiritin
445.1121	445.1129	−1.8	Glycitin
455.3541	455.3520	4.6	Trametenolic acid
635.4172	635.4154	2.8	Mongholicoside I
649.3954	649.3946	1.2	Astrolanosaponin C
783.4534	783.4536	−0.3	Astragaloside III
811.4841	811.4849	−1.0	Agroastragaloside V
825.4636	825.4642	−0.7	Astragaloside II
873.4849	873.4853	−0.5	Agroastragaloside II
911.5013	911.5009	0.4	Astragaloside VIII
945.5040	945.5065	−2.6	Astragaloside VI
953.5121	953.5115	0.6	Astroolesaponin F
987.5165	987.5170	−0.5	Agroastragaloside IV

LDA model was used to establish a multivariate statistical analysis, allowing the distinction of AR samples based on their molecular fingerprints. Figure 3b showed a three-dimensional PCA-LDA scatter plot, demonstrating complete separation and accurate distinction between WAR and CAR. All samples were clearly divided into two groups. The variance of a large group of inter-correlated variables, such as flavonoids and saponin species, was transformed into a small set of uncorrelated principal components (PCs). Bidimensional score plots along the first two main linear discriminants were shown in Fig. 3c, the sample distribution indicated that the two clusters were well separated along the PC2 axis. After the model was established, the cumulative variance contribution rate of the first two principal components was carefully studied to reveal the representative ions for sample classification. As shown in Fig. 3d, e, the contribution rates of PC1 and PC2 to chemical changes were 32.48% and 8.38%, respectively. The model is validated by "stratified 5-fold" validation, and model-building data is evenly divided into five partitions. Using four partitions (80%) of the data to build a model, while the remaining partition (20%) of the data is used to predict the classifications. This process is repeated five times, and each partition is predicted once by a model trained from the other four. Ultimately, the accuracy and generalization ability of the model are evaluated by counting the total number of correct and incorrect classifications, as well as the number of outliers. The output validation report detailed the total counts of correct and incorrect classifications, as well as the number of outliers identified. The results showed that within a comprehensive set of 314 mass spectra, there were three outliers, and a correct score of 99.04% was obtained (Fig. S3). These results showed that the model was stable, reliable, and statistically significant.

REIMS real-time recognition

The model constructed using reference AR samples was utilized for online identification of the collected unknown samples. LiveID software can quickly identify data and provides intuitive recognition results for each collected sample. Since the identification process was based on multi-target factor fingerprints, the software assesses the matching rate, and a 100% match confirms the sample's identity. To further ensure recognition accuracy, this experiment was designed such that if three out of ten chromatographic peaks have a recognition matching rate of 100%, this confirmed the sample was successfully matched. According to the established model, Fig. 3f, g showed representative recognition results of the decision and confidence level. A total of eight unknown samples were identified in real-time; samples U1-U4 were identified as WAR, and samples U5-U8 were identified as CAR. Recognition confidence for both WAR and CAR samples was above 99%. The results demonstrated that the REIMS-based method is also feasible and suitable for identifying WAR and CAR samples.

Compared with other identification methods, such as using a pseudotargeted metabolomics method to track AR relevant species from herbal products[31]. REIMS eliminates the need for sample pretreatment. It takes only a few seconds to complete data collection and analysis, avoiding the time-consuming analysis of traditional LC-MS. In addition, it can also generate information at the molecular level, and it is possible to identify different metabolite ions to distinguish medicinal materials. It provides a new approach for the analysis and identification of WAR and CAR, and is suitable for the analysis of TCMs.

2DLC-MS for validation

To further support the obtained results of the REIMS method, the 2DLC-MS combining HILIC and RPLC was applied. The high polar compounds were analyzed by the first-dimensional HILIC column. Subsequently, middle and low polar compounds that could not be separated were transferred to the second-dimensional RPLC column via a switching valve, which achieved good separation in a wide polar range. Chemical compounds from 20 batches of WAR and CAR were analyzed using the established 2DLC-MS method, with the representative TICs are shown in Fig. 4. By utilizing molecular formula prediction, online database retrieval, and the "assign" function in Insight Explore software, a total of 124 compounds were characterized, involving 40 flavonoids, 29 organic acids, 20 saponins and 35 others. The results of identification include compounds detected by REIMS. Detailed information about the retention time, high accurate precursor ions, molecular formulas, and major fragment ions of each compound are summarized in Table S2.

Multivariate statistical analysis of 2DLC-MS

To further investigate the differences in chemical components among WAR and CAR, chromatographic peaks from 20 batches obtained through 2DLC-MS in negative ion mode were subjected to MetaboAnalyst 6.0. The PCA scores for QC, WAR, and CAR are shown in Fig. 5a, showing a clear separation trend among the samples of each group, indicating significant differences between WAR and CAR. The QC samples were clustered

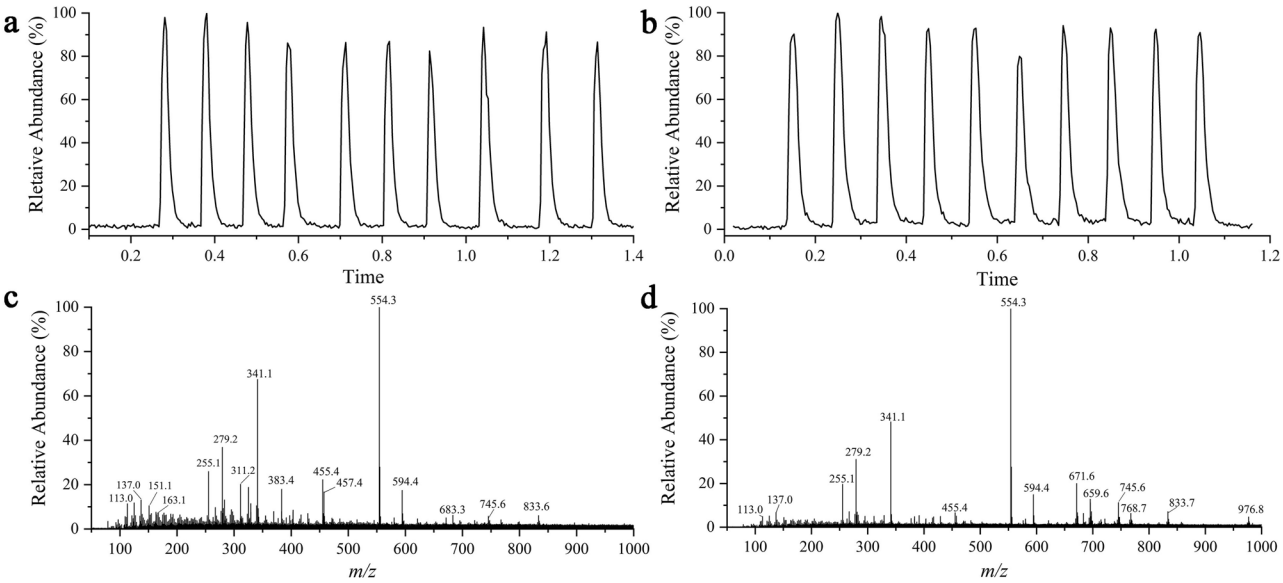

Fig. 2 | Representative TICs and mass spectra of WAR and CAR. a Representative TIC of WAR. **b** Representative TIC of CAR. **c** The mass spectra of WAR in the range of *m/z* 100–1000. **d** The mass spectra of CAR in the range of *m/z* 100–1000.

together, indicating no significant bias occurred during the measurement process, which suggests that the stability of the metabolomic data for both CAR and WAR was satisfactory. In order to obtain more prominent differences between two species and find potential markers, a supervised pattern recognition OPLS-DA model was performed (Fig. 5b). All the samples in the model were within 95% confidence interval, and the two groups of samples were completely separated without overlapping areas, showing obvious differences between WAR and CAR. R^2Y and Q^2 represent the model's interpretation rate and prediction ability, respectively. Values closer to 1 suggest a better model fit and higher credibility. With $R^2Y = 0.957$ and $Q^2 = 0.94$, indicating that the model was robust and reliable. The permutation test with 100 permutations was conducted to validate the effectiveness of OPLS-DA model. The results showed that the p was less than 0.01, indicating the model was not over-fitted (Fig. 5c). The volcano map (Fig. 5d) could conveniently and intuitively display the distribution of the difference expression between two samples. It indicates that statistical differences at points where the $p < 0.05$ and the fold change>2. Furthermore, based on VIP > 1.5, $p < 0.05$ and volcanic map, the potential markers of WAR and CAR were preliminarily screened out. Consequently, a total of 45 chemical compounds were screened out, corresponding to the compound details in Table S3.

Semi-quantitative analysis of 45 differential compounds between WAR and CAR

To further verify the above results, an MIM list containing 45 different compounds was finally established by recording the same precursor ions (Q_1) and fragment ions (Q_3). Subsequently, the MIM-IDA-EPI method was implemented to verify the reliability of the selected transition and further verify the results of chemical composition identification. The extraction ion chromatograms obtained by scanning 45 MIM transitions were shown in Fig. S4. Based on these compounds, the chromatographic peak area data of 40 batches of AR samples obtained from QTRAP. The 45 differential compounds, including organic acids, flavonoids, saponins, sucrose, and other compounds, were summarized in Table S3. Within the 19 differential organic acids, the contents of salicylic acid, vanillic acid, 2-isopropylmalic acid, ferulic acid, gluconic acid and 2-hydroxy-3,4-dimethylbenzoic acid were higher in CAR than in WAR. Conversely, the remaining organic acids were more abundant in WAR. Among the 14 differential flavonoids, 7,3',4'-trihydroxyflavone, glycitin, ononin, rhamnocitrin 3-*O*-neoheperoside and isomuconuratol 7,2'-di-O-β-glucoside were more abundant in CAR, while the levels of the other 9 flavonoids were higher in WAR. Calycosin, a significant flavonoid in AR, showed no significant difference in content between WAR and CAR. For saponin compounds, astragaloside II and astragaloside VI are key active components of AR, possessing anti-inflammatory property and enhancing neurological function[33,34]. The relative contents of these two saponins were higher in WAR compared to CAR, making WAR more advantageous for clinical applications. Notably, sucrose content in WAR was 28.45 ± 5.18, contrasting with the 35.31 ± 7.59 found in CAR, indicating obviously lower content in WAR. It may have application advantages in clinical application of WAR to treat diseases, especially diabetes. In conclusion, pronounced differences exist in the content of compounds between WAR and CAR, attributed primarily to variations in tissue structure and cell composition, as well as differences in cultivation methods and growth environments.

In this paper, the REIMS method was developed for the direct analysis of WAR and CAR samples. At the same time, combining 2DLC-MS and multivariate statistical model, the REIMS results were further verified, establishing their reliability. The proposed REIMS method could rapidly distinguish unknown AR samples with an accuracy of 99%. Through 2DLC-MS and multivariate statistical analysis, 45 different compounds were screened out and identified. Subsequently, based on the semi-quantitative analysis platform of UHPLC-QTRAP MS, a semi-quantitative method for 45 different compounds in WAR and CAR was established. Mainly consisting of organic acids, saponins and flavonoids, which could be considered as significantly differential metabolites between the two species. The results showed that the relative content of most compounds in WAR was higher than that in CAR. To summarize, the REIMS technique is a promising tool for low conductivity sample ionization and MS profiling without sample preparation. The strategy of this study not only provides an objective method for identifying WAR and CAR, but also provides a reference for the identification of other medicines with the same origin, so as to ensure the safety and effectiveness of their clinical use.

Materials and methods

Chemical and reagents

Formic acid, methanol, acetonitrile, ammonium acetate and leucine enkephalin (LC-MS grade) were provided by Fisher Scientific (Fair Lawn, NJ, USA), and distilled water vaporized at 105 °C was supplied by Watson's Food & Beverage Co., Ltd (Guangzhou, China). A total of 40 different

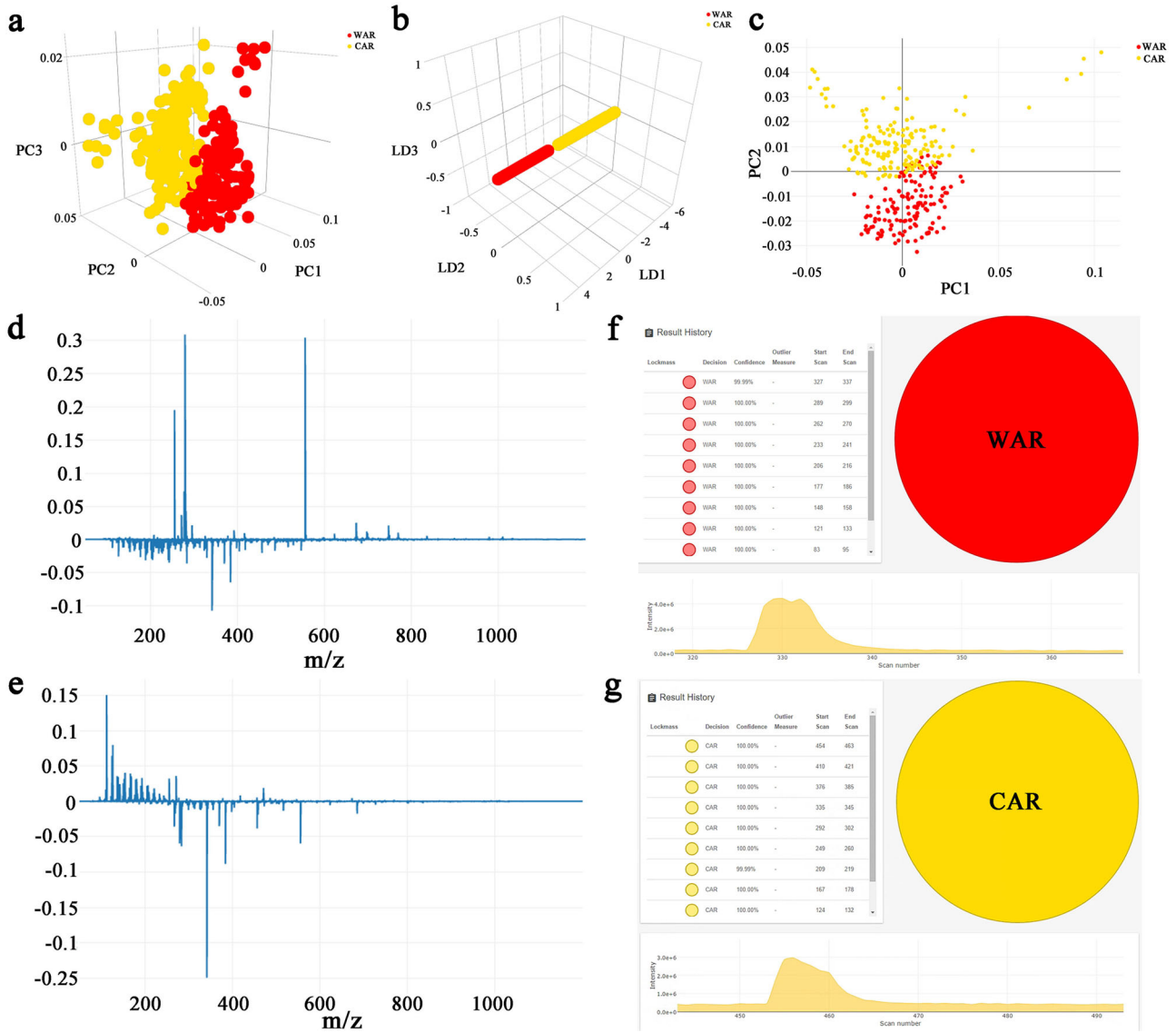

Fig. 3 | REIMS was used to model and identify the CAR and WAR. **a** Tridimensional visualization of PCA. **b** Tridimensional visualization of PCA-LDA. **c** Bidimensional score lots along the first two main linear discriminants. **d** Loading plot relative to the PC1. **e** Loading plot relative to the PC2 (explaining 32.48% and 8.38% of the total variance of the model). **f** Real-time recognition by LiveID of WAR in the mutivariate model. **g** Real-time recognition by LiveID of CAR in the mutivariate model.

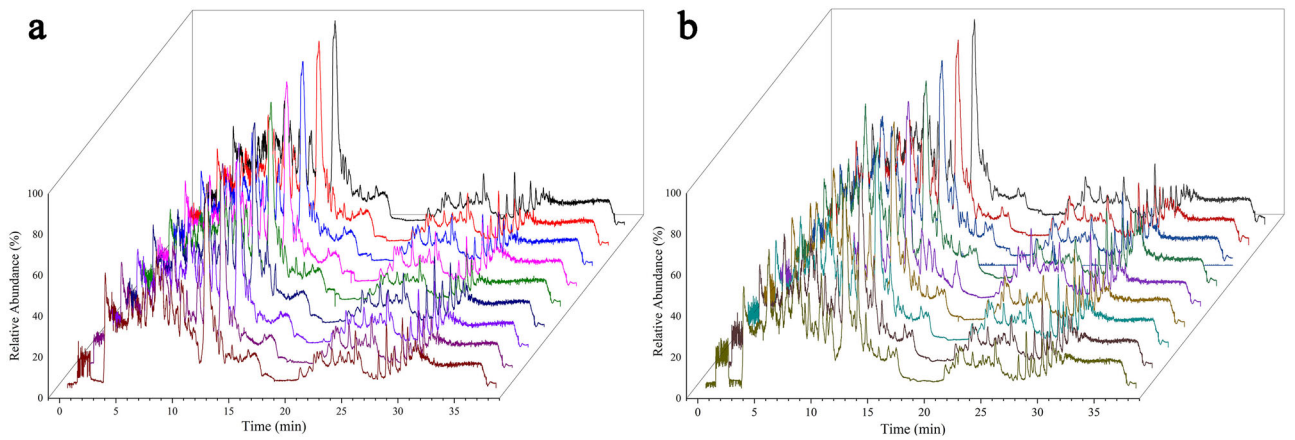

Fig. 4 | Waterfall diagram of representative TICs. **a** The TICs of WAR obtained by 2DLC-MS. **b** The TICs of CAR obtained by 2DLC-MS.

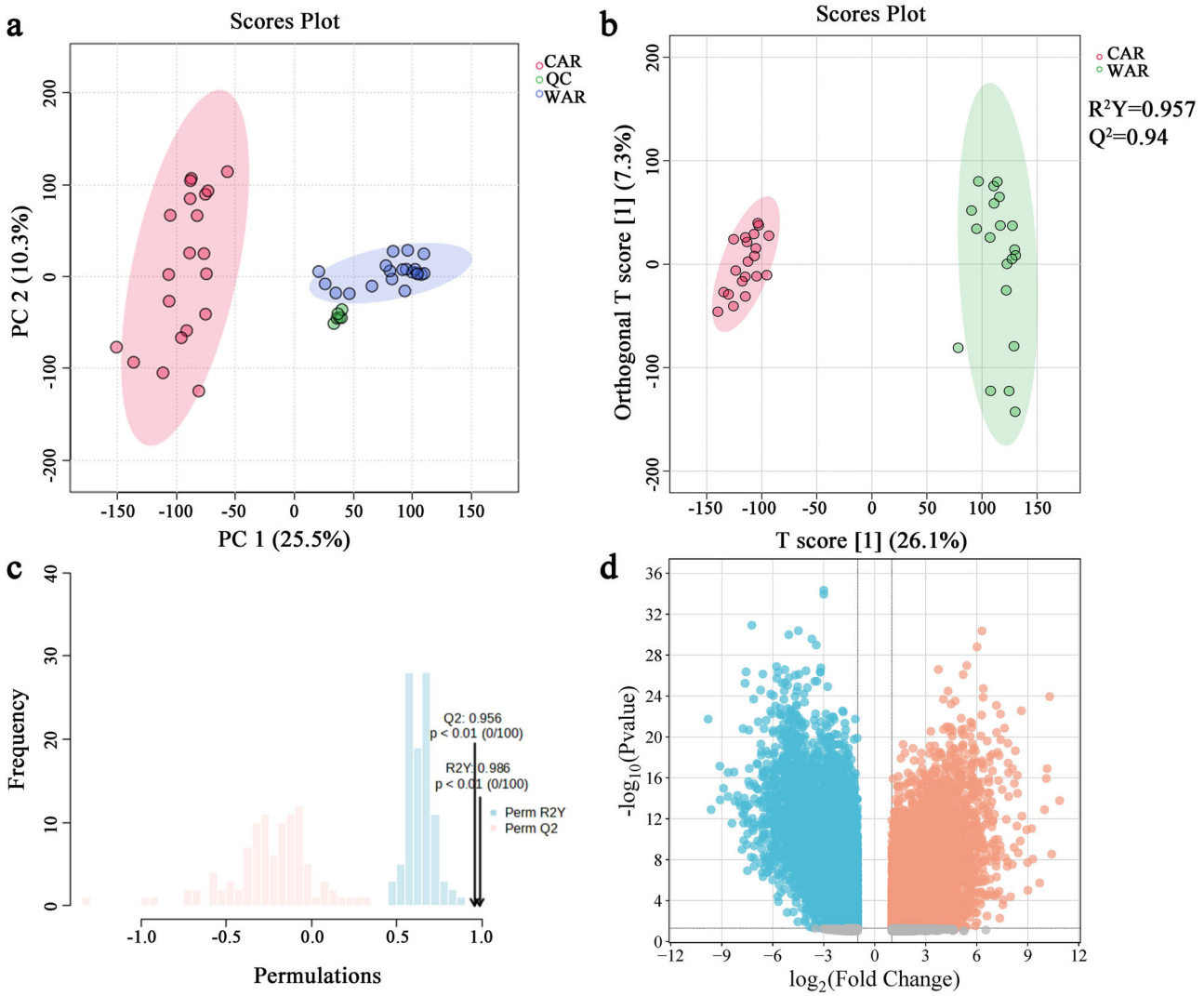

Fig. 5 | Multivariate statistical analysis of WAR and CAR to unveil differential ions. a Score plots of PCA. **b** Score plots of OPLS-DA. **c** Results of 100 permutation tests of OPLS-DA. **d** Volcano map.

batches of AR samples, including 20 batches WAR and 20 batches CAR, were shown in Table S4. These samples were subjected to authentication by Professor Pengfei Tu (Peking University, Beijing, China), and perform further confirmation based on microscopic structures. All these samples were deposited at the authors' laboratory (Peking University, Beijing, China).

Sample preparation

The sample was crushed and passed through a 50-mesh sieve. 1.0 g of powder was accurately weighed and added to 1.5 mL of water for dissolution, so that the sample became a certain viscous state, and the dissolved sample was placed into a cylindrical container wrapped with aluminum foil for testing, as shown in Fig. S5. Each batch of AR powder (1.0 g) was thoroughly mixed together to make a QC sample for the optimization of the REIMS experimental conditions.

Accurately weighed AR powder (500 mg) was placed into 15 mL centrifuge tubes containing 10 mL of 70% methanol (*v*/*v*). Then the samples were ultrasonic extracted for 1 h, followed by centrifugation at 10,000 rpm for 10 min, and the supernatant was passed through a 0.22 μm polytetrafluoroethylene (PTFE) membrane to be detected by 2DLC-MS. A QC sample was prepared by mixing equal volumes of each AR sample to evaluate the performance of the 2DLC-MS system. All sample solutions were stored in a refrigerator at 4 °C before use.

REIMS analysis

The REIMS analysis was performed using a REIMS ion source coupled to a Waters Xevo G2-XS quadrupole time-of-flight mass spectrometer (Waters, Milford, MA). In this study, a monopolar electrosurgical knife (Model PS01-63H, Hangzhou medstar technology Co, Ltd, Jiaxing City, China) device was used to apply localized high-frequency current to the surface of the samples through a 3 m long, 1 cm diameter ultra-flexible tubing (evacuation/vent line). Electrosurgical dissection in all experiments was performed using an Erbe VIO 50 C generator (Erbe Medical UK Ltd, Leeds, UK). Each sample was burned, and the aerosols containing gaseous compounds were aspirated through a PTFE tube attached to a venturi gas jet pump that is attached to the REIMS source described above. The ionization conditions of the iKnife were optimized as follows: heater bias voltage: 55 V; cutting time: 1 S; cutting length: 1 cm; cone voltage: 40 V. Ten technical replicates were carried out per sample with 2–3 s delay between each cut. 0.1% formic acid-50% acetonitrile/water (*v*/*v*) of leucine enkephalin solution (200 pg/μL) was used as a lock mass solution and continuously introduced at a flow rate of 2 μL/min. The mass spectra were acquired in negative ion mode with the mass range of *m*/*z* 50–1200.

2DLC-MS analysis

The 2DLC-MS system was constructed by a Nexera X2 system (Shimadzu, Kyoto, Japan) equipped with two binary high-pressure gradient pumps

(LC-30AD), a secondary array detector (SPD-M20A), a system controller (CBM-20A), an automatic sample injector (SIL-30 AC), a column oven (CTO-20 AC), a 500 μL sample loop and a 10-port switching valve. The mass detector was a time-of-flight mass spectrometer (LCMS 9030) (Shimadzu Corporation, Japan) with an electrospray ionization source. Labsolutions software (Ver. 5.118) was used for data acquisition and control of the system. A SeQuant® ZIC®-cHILIC (150 × 2.1 mm, 3 μm, Merck, Germany) was used in the first dimensional hydrophilic interaction chromatography (HILIC) mode and a Kinetex C8 (150 × 2.1 mm, 2.6 μm, Phenomenex, USA) was used in the second dimensional reversed-phase liquid chromatography (RPLC) mode. The first dimensional liquid phase conditions were as follows: mobile phase A_1, 5 mM ammonium acetate-0.1% formic acid/water; mobile phase B_1, 5 mM ammonium acetate-acetonitrile; flow rate, 0.3 mL/min; column temperature, 40 °C. The second dimension liquid phase conditions: mobile phase A_2, 2 mM ammonium acetate-0.1% formic acid/water; mobile phase B_2, acetonitrile; flow rate, 0.3 mL/min; column temperature, 40 °C; injection volume, 2 μL. The optimized 2DLC gradient elution procedures and the switching valve time are listed in Table S5. For MS conditions, data acquisition was performed using the data-dependent acquisition mode, with 6 scanning events in each mode and the mass range of *m/z* 50–1200. The detailed parameters about 2DLC-MS are listed in Table S6.

UHPLC-QTRAP analysis

UHPLC analysis was performed using a Shimadzu LC-20AD system (Shimadzu, Kyoto, Japan). Chromatographic separation was performed on a Waters ACQUITY UPLC™ BEH C18 column (2.1 × 100 mm, 1.7 μm). The mobile phase consists of 0.1% formic acid/water (A) and acetonitrile (B) at a flow rate of 0.3 mL/min. The injection volume was 2 μL and the temperature for the column oven was set at 35 °C. The programmed elution procedure of UHPLC is listed in Table S7. MS analysis was performed on a QTRAP 4500 equipped with an ESI source (AB SCIEX, Framingham, MA, USA). The relevant parameters of MS are given in Table S6. MIM refers to the technique of simultaneously monitoring multiple target ions, allowing for the selective capture of signals from multiple ions within a specific time window. Semi-quantitative methods of 45 different compounds were established based on MIM scanning mode, and suitable Q_1 and Q_3 ions of compounds were obtained by MIM-information dependent acquisition-enhanced product ion (MIM-IDA-EPI) mode. Table S8 detailed the information for 45 compounds set in MIM-IDA-EPI.

Data processing and analysis

MassLynx 4.2 (Waters, Milford, USA) was used for REIMS data acquisition and peak extraction, and all MS data was collected in negative ion mode. The mass spectra signals of 10 peaks were taken from each sample to build a model. Data analysis was completed by LiveID 1.2 software (Waters, Milford, MA). The setting parameters for "Build the model" in Live ID are as follows: five PCA components; one linear discriminant; three standard deviations; binning resolution of 0.1 *m/z*; mass range of 50–1200 *m/z*. Using the default Leu-Enk setting for the demonstration data. For 2DLC data, peak extraction and alignment were achieved using MS-DIAL 5.1.230912 software. The setting parameters related to data processing by MS-DIAL software are as follows: MS1 tolerance, 0.01 Da; MS2 tolerance, 0.025 Da; minimum peak height, 1000 amplitude; mass slice width: 0.1 Da; retention time tolerance, 0.1 min. The compounds were identified by molecular formula prediction, online database retrieval (ChemSpider/PubChem), and confirmation using the "assign" function in Insight Explore software (Shimadzu, Kyoto, Japan). MetaboAnalyst 6.0 was used for statistical analysis, including principal component analysis (PCA) and orthogonal partial least squares discriminant analysis (OPLS-DA). The related parameters settings are as follows: missing value estimation, remove features with >50 missing values; sample normalization, normalization by sum; data transformation, log transformation; data scaling, pareto scaling. Subsequently, supervised OPLS-DA analysis was used to visualize the variable difference between two groups, and 100 permutation test was conducted to avoid over-fitting of OPLS-DA model. Metabolites with a variable importance to the projection value (VIP) > 1.5 and *p*-value (p) < 0.05 were considered as differential metabolites. The raw QTRAP data was controlled and analyzed by Analyst 1.6.2 (AB SCIEX, Framingham, MA, USA) software.

Data Availability

All data generated or analysed during this study are included in this published article and its supplementary information files.

Received: 14 August 2024; Accepted: 28 October 2024;
Published online: 08 November 2024

References

1. Fu, J. et al. Review of the botanical characteristics, phytochemistry, and pharmacology of *Astragalus membranaceus* (Huangqi). *Phytother. Res.* **28**, 1275–1283 (2014).
2. Chen, Z. et al. Astragali Radix (Huangqi): a promising edible immunomodulatory herbal medicine. *J. Ethnopharmacol.* **258**, 112895 (2020).
3. Chang, X. et al. Advances in chemical composition, extraction techniques, analytical methods, and biological activity of astragali radix. *Molecules* **27**, 1058 (2022).
4. Wang, X. et al. Study on genetic diversity of *Astragalus membranaceus* var. *mongholicus* populations in inner Mongolia. *Chin. J. Grassl.* **40**, 42–48 (2018).
5. Hu, M. et al. Quality analysis of semi-cultivated *Astragalus membranaceus* var. *mongholicus* from Hunyuan County of Shanxi Province. *Chin. Traditional Herb. Drugs* **43**, 1829–1834 (2012).
6. Guo, X., Lin, H., Xu, S. & He, L. Recent advances in spectroscopic techniques for the analysis of microplastics in food. *J. Agric. Food Chem.* **70**, 1410–1422 (2022).
7. Lapidot-Cohen, T., Rosental, L. & Brotman, Y. Liquid Chromatography-Mass Spectrometry (LC-MS)-based analysis for lipophilic compound profiling in plants. *Curr. Protoc. Plant Biol.* **5**, e20109 (2022).
8. Longo, V., Forleo, A., Giampetruzzi, L., Siciliano, P. & Capone, S. Human biomonitoring of environmental and occupational exposures by GC-MS and gas sensor systems: a systematic review. *Int. J. Environ.* **18**, 10236 (2021).
9. Pietruk, M., Jedziniak, P. & Olejnik, M. LC-MS/MS determination of 21 non-steroidal anti-inflammatory drugs residues in animal milk and muscles. *Molecules* **26**, 5892 (2021).
10. Fu, Y. et al. Nontargeted screening method for illegal additives based on ultrahigh-performance liquid chromatography-high-resolution mass spectrometry. *Anal. Chem.* **88**, 8870–8877 (2016).
11. Elbaz, G. A., Zaazaa, H. E., Monir, H. H. & Abd El Halim, L. M. Chitosan nanoparticles modified TLC-densitometry for determination of imidacloprid and deltamethrin residues in plants: greenness assessment. *BMC Chem.* **17**, 29 (2023).
12. Zhang, X. et al. Identification strategy of Fructus Gardeniae and its adulterant based on UHPLC/Q-orbitrap-MS and UHPLC-QTRAP-MS/MS combined with PLS regression model. *Talanta* **267**, 125136 (2024).
13. Zhang, K. et al. Integrated widely targeted metabolomics and network pharmacology revealed quality disparities between Guizhou and conventional producing areas of Codonopsis Radix. *Front. Nutr.* **10**, 1271817 (2023).
14. Balog, J. et al. Intraoperative tissue identification using rapid evaporative ionization mass spectrometry. *Sci. Transl. Med.* **5**, 194ra93 (2013).
15. Jones, E. A. et al. Matrix assisted rapid evaporative ionization mass spectrometry. *Anal. Chem.* **91**, 9784–9791 (2019).
16. He, Q. et al. Differentiation between fresh and frozen-thawed meat using rapid evaporative ionization mass spectrometry: the case of beef muscle. *J. Agr. Food Chem.* **69**, 5709–5724 (2021).
17. Song, G. et al. Real-time in situ screening of Omega-7 phospholipids in marine biological resources using an iknife-rapid-evaporative-

ionization-mass-spectrometry-based lipidomics phenotype. *J. Agr. Food Chem.* **69**, 9004–9011 (2021).
18. Mangraviti, D. et al. Rapid evaporative ionization mass spectrometry-based lipidomics for identification of canine mammary pathology. *Int. J. Mol. Sci.* **23**, 10562 (2022).
19. Phelps, D. L. et al. The surgical intelligent knife distinguishes normal, borderline and malignant gynaecological tissues using rapid evaporative ionisation mass spectrometry (REIMS). *Br. J. Cancer* **118**, 1349–1358 (2018).
20. St John, E. R. et al. Rapid evaporative ionisation mass spectrometry of electrosurgical vapours for the identification of breast pathology: towards an intelligent knife for breast cancer surgery. *Breast Cancer Res.* **19**, 59 (2017).
21. Paraskevaidi, M. et al. Laser-assisted rapid evaporative ionisation mass spectrometry (LA-REIMS) as a metabolomics platform in cervical cancer screening. *eBioMedicine* **60**, 103017 (2020).
22. Shen, Q. et al. Detection of lipidomics characterization of tuna meat during different wet-aging stages using iKnife rapid evaporative ionization mass spectrometry. *Food Res. Int.* **156**, 111307 (2022).
23. De Graeve, M. et al. Multivariate versus machine learning-based classification of rapid evaporative Ionisation mass spectrometry spectra towards industry based large-scale fish speciation. *Food Chem.* **404**, 134632 (2023).
24. Lu, W. et al. Real-time authentication of minced shrimp by rapid evaporative ionization mass spectrometry. *Food Chem.* **383**, 132432 (2022).
25. Kelis Cardoso, V. G., Sabin, G. P. & Hantao, L. W. Rapid evaporative ionization mass spectrometry (REIMS) combined with chemometrics for real-time beer analysis. *Anal. Methods* **14**, 1540–1546 (2022).
26. Qiao, X. et al. Separation and detection of minor constituents in herbal medicines using a combination of heart-cutting and comprehensive two-dimensional liquid chromatography. *J. Chromatogr. A* **1362**, 157–167 (2014).
27. Ma, S. et al. A simple way to configure on-line two-dimensional liquid chromatography for complex sample analysis: acquisition of four-dimensional data. *Talanta* **97**, 150–156 (2012).
28. Zhou, W. et al. Application of two-dimensional liquid chromatography in the separation of traditional Chinese medicine. *J. Sep. Sci.* **43**, 87–104 (2020).
29. Chang, K. et al. Identification and characterization of quinoline alkaloids from the root bark of Dictamnus dasycarpus and their metabolites in rat plasma, urine and feces by UPLC/Qtrap-MS and UPLC/Q-TOF-MS. *J. Pharm. Biomed. Anal.* **204**, 114229 (2021).
30. Wang, X. et al. Pseudotargeted metabolomics approach enabling the classification-induced ginsenoside characterization and differentiation of ginseng and its compound formulation products. *J. Agric. Food Chem.* **71**, 1735–1747 (2023).
31. Cai, W. L. et al. Pseudotargeted metabolomics-based random forest model for tracking plant species from herbal products. *Phytomedicine* **118**, 154927 (2023).
32. Zhao, D. et al. A multidimensional chromatography/high-resolution mass spectrometry approach for the in-depth metabolites characterization of two Astragalus species. *J. Chromatogr. A* **1688**, 463718 (2023).
33. Qiao, C. et al. Astragaloside II alleviates the symptoms of experimental ulcerative colitis in vitro and in vivo. *Am. J. Transl. Res.* **11**, 7074–7083 (2019).
34. Chen, X. et al. Astragaloside VI promotes neural stem cell proliferation and enhances neurological function recovery in transient cerebral ischemic injury via activating EGFR/MAPK signaling cascades. *Mol. Neurobiol.* **56**, 3053–3067 (2019).

Acknowledgements

This work was supported by the National Key R&D Program of China (No. 2022YFC3501600), and the National Natural Science Foundation of China (No. 82030114, 82104543 and 22177005).

Author contributions

Sijian Chen: Investigation, Writing-original draft, Formal analysis. Xiaoshuang Li: Formal analysis, Visualization. Danshu Shi: Data curation, Visualization. Yisheng Xu: Data curation, Visualization. Yingyuan Lu: Supervision, Conceptualization, Writing-review & editing. Pengfei Tu: Supervision, Writing- review & editing, Project administration.

Competing interests

The authors declare no competing interests.

Additional information

Supplementary information The online version contains supplementary material available at https://doi.org/10.1038/s41538-024-00333-3.

Correspondence and requests for materials should be addressed to Yingyuan Lu or Pengfei Tu.